

Polar derivatives of the $[closo-1-CB_9H_{10}]^-$ cluster as positive $\Delta\epsilon$ additives to nematic hosts†

Bryan Ringstrand,^a Piotr Kaszynski,^{*,a} Adam Januszko^a and Victor G. Young, Jr.^b

Received 9th July 2009, Accepted 26th September 2009

First published as an Advance Article on the web 26th October 2009

DOI: 10.1039/b913701g

Polar ($\mu \approx 16$ D) and UV transparent >250 nm quinuclidinium (**1**) and sulfonium (**2**) zwitterionic derivatives of the $[closo-1-CB_9H_{10}]^-$ anion were synthesized and studied as additives to nematic hosts. The molecular and crystal structures for **1** [$C_{19}H_{44}B_9N$ triclinic, P-1, $a = 9.766(2)$ Å, $b = 10.481(3)$ Å, $c = 12.098(3)$ Å, $\alpha = 93.804(9)^\circ$, $\beta = 90.249(10)^\circ$, $\gamma = 102.587(10)^\circ$, $Z = 2$] were determined by X-ray crystallography and compared with the results of HF/6-31G(d) calculations. Low concentration solutions (<10 mol%) of **1** and **2** in **CI Ester** host ($\Delta\epsilon = -0.59$) were investigated using thermal and dielectric methods. The results for **1** and **2** showed virtual $[T_{NI}]$ values of 139 °C and 92 °C, and $\Delta\epsilon$ extrapolated to infinite dilution of 70 ± 1 and 61 ± 2 , respectively. Dielectric results were analyzed using the Maier-Meier relationship and calculated molecular parameters. The apparent order parameter S_{app} was found to be 0.63 and 0.50 for **1** and **2**, respectively, which is smaller than that for the pure host ($S = 0.66$). Analysis of the Kirkwood factors g obtained for each concentration gave an association constant K of 63 ± 2 and 37 ± 1 (model 1) for the assumed dimerization of molecules ($2M \rightleftharpoons M_2$) of **1** and **2**, respectively, in solutions of **CI Ester**.

Introduction

Nearly all liquid crystal (LC) electrooptical devices, such as flat panel displays,^{1,2} rely on the so-called Fréedericksz transition,³ where polar oriented molecules re-orientate in an external electric field resulting in a change of the optical properties of the bulk material.^{4,5} The threshold voltage (V_{th}) for the reorientation of the LC molecules is inversely proportional to the square root of dielectric anisotropy, $\Delta\epsilon$, which in turn is proportional to the molecular dipole moment and its orientation relative to the main molecular axis, $\sim\mu^2(1 - 3\cos^2\beta)$. Therefore, the larger the dipole moment, the lower the threshold voltage ($V_{th} \sim 1/\mu$).

Liquid crystals with positive dielectric anisotropy ($\Delta\epsilon > 0$) are typically designed by using polar terminal substituents, such as $-CN$,⁶ $-NCS$,⁷ and F ,² or heterocycles, such as pyrimidine⁸ or dioxane,⁹ as part of the rigid core, with the net dipole moment oriented along the long molecular axis.^{2,10,11} Dipole moments associated with these molecular fragments are moderate and generally do not exceed 5 D (e.g., for benzonitrile¹² $\mu = 4.52$ D). Much larger molecular dipole moments are observed for zwitterions,¹³ and for some compounds values near 16 D have been measured.^{14,15} Anisometric compounds (elongated molecular shapes) possessing such large dipole moments could serve as

effective low-concentration polar additives that significantly increase $\Delta\epsilon$ of the liquid crystalline material. However, most zwitterions have geometries incompatible with a typical nematic LC material, which limits their usefulness in electrooptical applications. To date only three classes of zwitterionic mesogens, pyrazo[1,2-*a*]pyrazoliumolates,¹⁶ syndones,¹⁷ and *N*-pyridinium-4-alkoxybenzamides,¹⁸ have been reported but their compatibility with nematic materials has not been investigated. A class of zwitterions that are particularly attractive for the design of polar mesogens or additives to nematic materials is based on monocarbaborates **A** and **B** (Fig. 1).^{19–21}

closo-Monocarbaborates $[closo-1-CB_9H_{10}]^-$ and $[closo-1-CB_{11}H_{12}]^-$ (**A** and **B**, Fig. 1) belong to an extensive family of *closo*-boranes, which are characterized by sigma-aromaticity and complete negative charge delocalization.²¹ The geometry of the two clusters, **A** and **B**, appears to be appropriate for the formation of calamitic liquid crystals, as is indicated by results for their electrically neutral isostructural *p*-carborane analogues.^{22–26} Extensive experimental data demonstrate that

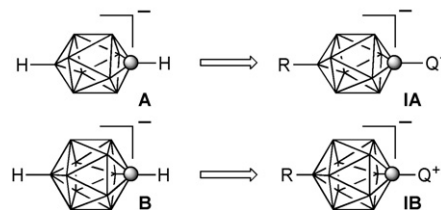


Fig. 1 The structures of the ionic $[closo-1-CB_9H_{10}]^-$ and $[closo-1-CB_{11}H_{12}]^-$ clusters (**A** and **B**), and their polar derivatives (**IA** and **IB**). Each vertex represents a BH fragment, the sphere is a carbon atom, and Q^+ stands for an onium group such as an ammonium, sulfonium, or pyridinium.

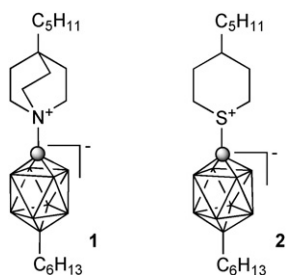
^aOrganic Materials Research Group, Department of Chemistry, Vanderbilt University, Nashville, TN, 37235, USA

^bX-ray Crystallographic Laboratory, Department of Chemistry, University of Minnesota, Twin Cities, MN, 55455, USA

† Electronic supplementary information (ESI) available: synthetic details and characterization data for compounds **1**, **2**, **4**, **5**, **8**, and **10**, details of dielectric data, dielectric analysis, crystal data collection information, selected experimental and theoretical geometrical parameters for **1** and **2**, archive of calculated equilibrium geometries for **1** and **2**. CCDC reference number 731853. For ESI and crystallographic data in CIF or other electronic format see DOI: 10.1039/b913701g

both *p*-carboranes support liquid crystalline phase formation, and their derivatives strongly prefer the nematic over smectic phases. Therefore, clusters **A** and **B** substituted in the antipodal positions with appropriate groups are expected to exhibit an LC state or at least be compatible with the nematic phase. The use of an onium fragment, Q^+ , as one of the substituents introduces a substantial dipole moment oriented along the long molecular axis (Fig. 1). Our previous calculations²¹ demonstrated that the dipole moment expected from such derivatives of clusters **A** and **B** can exceed 15 D, which is difficult to obtain in organic non-zwitterionic species.

The unique properties of *closo*-boranes and opportunities to engineer highly polar and oriented materials for electrooptical applications prompted us to investigate the two monocarbaborates **A** and **B** as the centerpiece of rod-like compounds **IA** and **IB** (Fig. 1). In this paper, we focus on the 10-vertex system, the [*closo*-1-CB₉H₁₀]⁻ anion **A**. We establish the method for the introduction of alkyl and appropriate onium fragments into the {*closo*-1-CB₉} cage and prepare the first two such derivatives, **1** and **2**, from isomerically pure iodo acid²⁷ [*closo*-1-CB₉H₈-1-COOH-10-I]⁻. We investigate both derivatives as additives to nematic hosts, and study such binary mixtures by thermal and dielectric methods. The dielectric data are analyzed with the aid of the Maier-Meier relationship, which uses molecular parameters derived from quantum-mechanical calculations. Finally, we quantify the behavior of **1** and **2** in the nematic solution by deriving the association constant *K* from the dielectric data.



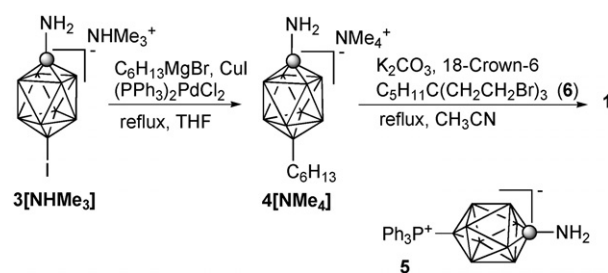
Results

Synthesis

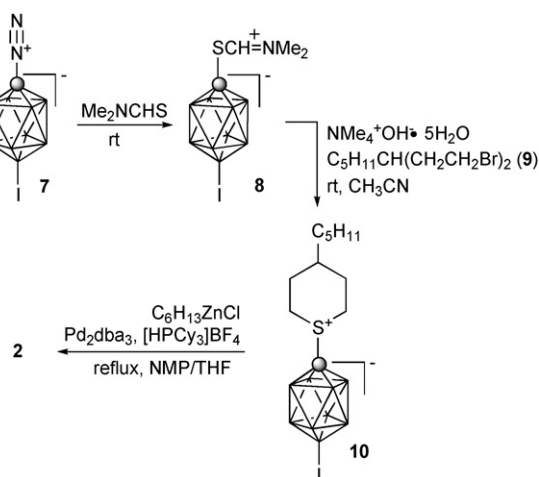
Derivatives **1** and **2** were prepared starting from iodo amine²⁸ **3** by a combination of alkylative cyclization at the C(1) vertex and Pd(0) catalyzed coupling at the B(10) vertex.

For quinuclidinium derivative **1**, iodo amine **3**[NHMe₃] was reacted with excess hexylmagnesium bromide in the presence of CuI and Pd(0) giving hexyl amine **4**[NMe₄] in 33% yield. Phosphonium adduct **5** was isolated as a by-product in 20% yield and partially characterized. The formation of an adduct similar to **5** was also observed in the Pd-catalyzed hexylation of iodo acid [*closo*-1-CB₉H₈-1-COOH-10-I]⁻ NMe₄⁺ using tricyclohexylphosphine as a ligand.²⁸ Alkylation of amine **4**[NMe₄] with tribromide²⁹ **6** in the presence of a base under phase-transfer catalysis conditions gave quinuclidinium derivative **1** in 33% yield (Scheme 1).

The introduction of the sulfonium fragment at the C(1) vertex and formation of **2** was envisioned by using a dinitrogen



Scheme 1



Scheme 2

functionality in analogy to the preparation of [*closo*-1-CB₉H₉-1-SC₅H₁₀] from [*closo*-1-CB₉H₉-1-N₂].³⁰ Our initial experiments with diazotization of hexyl amine **4**[NMe₄] demonstrated that the corresponding dinitrogen derivative [*closo*-1-CB₉H₈-1-N₂-10-C₆H₁₃] was an unstable oil that was difficult to purify and handle. Therefore, we focused on iodo dinitrogen derivative **7**, which we previously prepared in high yield from amine **3** and isolated as a stable, crystalline solid, suitable for further synthetic transformations.²⁸ Thus, the dinitrogen derivative **7** was reacted at ambient temperature with Me₂NCHS to form protected mercaptan **8**, which upon reactions with dibromide³¹ **9** under hydrolytic conditions gave sulfonium derivative **10** in 39% overall isolated yield. The hexyl group was introduced at the B(10) position by reacting **10** with hexylzinc chloride under Negishi conditions, previously used for the hexylation of iodo acid²⁸ [*closo*-1-CB₉H₈-1-COOH-10-I]⁻ NMe₄⁺, giving sulfonium derivative **2** in 58% yield (Scheme 2).

Thermal properties

Calorimetric (DSC) and optical (POM) analyses revealed that both polar derivatives **1** and **2** are high melting solids (>200 °C) and neither forms liquid crystalline phases. DSC demonstrated two transitions for each compound corresponding to a Cr–Cr transition and melting (Table 1). The solid–solid transition in quinuclidinium **1** is a high energy, broad peak spread over 40 K with a maximum at 126 °C. The melting at 363 °C has a similar high endotherm and is accompanied by rapid decomposition. The analogous transitions for the sulfonium **2** occur at lower

Table 1 Transition temperatures (°C) and enthalpies (kJ/mol in parentheses) for **1** and **2**^a

1		2	
Cr ₁ 109 (21.6)	Cr ₂ 363 (19.0)	I (dec)	Cr ₁ 66 (21.1)
			Cr ₂ 209 (10.9)

^a Cr = crystal, I = isotropic. ^b A second Cr–Cr transition at 86 °C (2.3 kJ/mol) was observed in an aged sample.

temperatures at which the compound is thermally stable. An additional transition at 86 °C (2.3 kJ/mol) was detected in a one-year-old sample of **2**. After heating this sample to 150 °C followed by conditioning at ambient temperature for 5 hrs the transitions at 66 °C and 86 °C were replaced with new transitions at 55 °C and 77 °C, respectively. After 20 hrs at ambient temperature the original transition at 66 °C partially reappeared in addition to the other two transitions. The isotropic phase of **2** supercools by 12 K before crystallization.

POM observations of samples of **1** and **2** revealed practically no change in the appearance of the crystals at the solid–solid transitions.

Electronic absorption

Spectroscopic analysis demonstrated that both compounds are practically transparent above 250 nm (Fig. 2). The quinuclidinium **1** and sulfonium **2** have high-energy absorption bands with the maximum at 204.5 nm and 210 nm, respectively, and with a shoulder feature at about 230 nm. The spectra recorded for **1** and **2** are similar to those obtained for [1-*closo*-CB₉H₉-1-NMe₃]³⁰ and [1-*closo*-CB₉H₉-1-SMe₂]³⁰ with the absorption bands shifted to lower energies (10 nm for **2**) presumably due to the presence of the alkyl group at the B(10) position.

Molecular and crystal structures

Colorless, triclinic crystals of **1** were grown from a toluene/*iso*-octane mixture by slow evaporation. The solid-state structure for

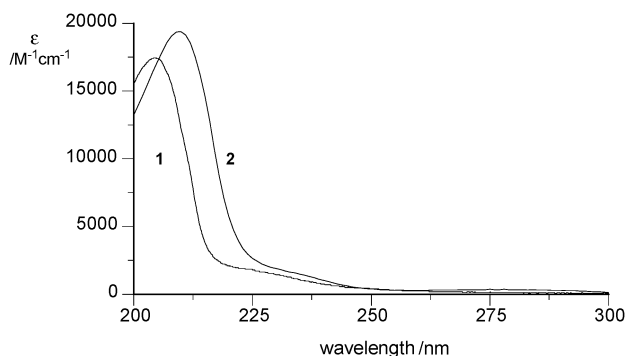


Fig. 2 Electronic absorption spectra of **1** and **2** recorded in MeCN.

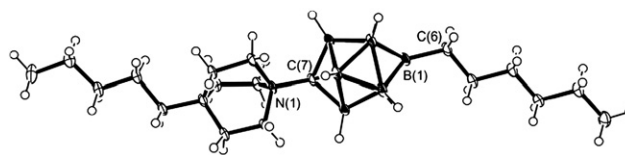


Fig. 3 Thermal ellipsoid diagram representation of quinuclidinium **1** drawn at 50% probability. Pertinent interatomic dimensions: C(7)–N(1) 1.505(2) Å, C(6)–B(1) 1.593(3) Å, avg B–C(7) 1.619 Å, avg B–B(1) 1.715 Å, C–N(1) avg 1.525 Å. Quinuclidine cage twist avg 18.8°.

1 was determined by X-ray diffraction³² and pertinent interatomic dimensions are shown in Fig. 3.

Crystallographic analysis revealed that the unit cell is occupied by two identical molecules of **1**, that are related through an inversion center. The separation between the long axes of the molecules in the unit cell is about 5.8 Å. In the crystal structure, molecules of **1** form infinite sheets perpendicular to the *ab* plane with alternating antiparallel arrangement.

In a molecule of **1**, the C(7)–N(1) distance between the quinuclidine ring and the {*closo*-1-CB₉} cage is 1.505(3) Å and the average B–C(7) distance is 1.619 Å. These distances are slightly longer by 0.007 Å and 0.011 Å, respectively, than those reported for the analogous trimethylamino derivative [1-*closo*-CB₉H₉-1-NMe₃].³³ Similar differences are observed in the pair of 1-quinuclidine and 1-NMe₃ derivatives of the {*closo*-1-CB₁₁} cluster.³⁴ The quinuclidine ring in **1** is twisted by an average value of 18.8°, which is larger than the average value of 8.3° found in a similar derivative of {*closo*-1-CB₁₁}.³⁴ This is presumably due to the shorter C_{cage}–N distance in the former than in the latter compound. The pyramidalization angle³⁵ α of the nitrogen atom in the quinuclidine ring is 21.2°, which is practically the same as in the quinuclidinium derivative of the {*closo*-1-CB₁₁}³⁴ and also in the quinuclidine–1-boraadamantane complex.³⁶

The dimensions of the {*closo*-1-CB₉} cage are similar to those reported for [1-*closo*-CB₉H₉-1-NMe₃].³³ Both alkyl groups are in all-*trans* conformation with dihedral angles little deviating from the ideal 180°. The largest deviation from planarity is observed for the pentyl group in which the angle defined by C _{α} –C _{β} –C _{γ} –C _{δ} is 166°. The two alkyl groups, the hexyl and the pentyl, deviate from the ideal staggered conformations with the {*closo*-1-CB₉} cage and quinuclidine ring by about 10° and 8°, respectively. Also, the orientation of the quinuclidine ring relative to the {*closo*-1-CB₉} cage is about 6° off the ideal staggered conformation.

The angle between the two alkyl chain planes in **1**, as defined by C _{α} –C _{β} –C _{γ} in each chain, is 11°.

Computation of molecular properties

The experimental structure of **1** is well reproduced by the HF/6-31G(d) level calculations.³⁷ The quinuclidine and the {1-*closo*-CB₉} cage adopt an eclipsed conformation in the ground state (Fig. 4), which is consistent with the solid state structure of [1-*closo*-CB₉H₉-1-Me₃N].³³ In contrast, in **1** the two rings are 8.6° away from the eclipsed conformation, presumably to minimize the inter-planar angle between the two alkyl chains.

The alkyl chains prefer pseudo-staggered conformations relative to the cage and the ring, which results in 22° angle between the alkyl group planes, each defined by the C _{α} –C _{β} –C _{γ} atoms, in

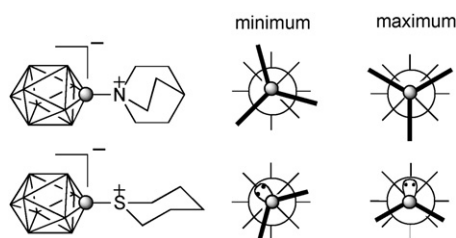


Fig. 4 Extended Newman projection along the long molecular axes of **1** and **2** showing main conformations. The bars represent the substituent and the circle is the nitrogen or sulfur atom.

the global conformational minimum of **1**. Similar conformational preferences are found in sulfonium **2** in which the sulfur atom lone pair eclipses the C–B bond. The orientation of the pentyl chain is staggered with respect to the thiacyclohexane ring, which results in a wider interplanar angle between the alkyl chains (41°), and consequently less linear molecular shape than that of **1** in the global conformational minimum.

The HF level calculations demonstrated a substantial longitudinal dipole moment, μ_{\parallel} , exceeding 15 D for both molecules (Table 2). The transverse component of the dipole, μ_{\perp} , is small, which results in a nearly parallel orientation of the net molecular dipole along the long molecular axes ($\beta = 9^\circ$). The magnitude and, to some degree, orientation of the dipole moment in **1** and **2** depend on the strength of the dielectric medium. IPCM calculations revealed an approximately linear dependence of the dipole moment in **1** and **2** on ϵ of the medium in the range of $\epsilon = 1$ (vacuum) to $\epsilon = 4.6$.³⁷

Polarizability tensors α for **1** and **2** were obtained using the B3LYP method. Results shown in Table 2 demonstrate that polarizability α and its anisotropy, $\Delta\alpha$, calculated for both compounds are consistent with those for typical two-ring liquid crystalline compounds.³⁸

Binary mixtures

Both zwitterions exhibited low solubility in nematic hosts containing a significant fraction of aliphatic groups. Thus, mixtures

Table 2 Calculated molecular parameters for **1** and **2**^a

	1	2
μ_{\parallel}/D	15.9	15.3
μ_{\perp}/D	2.9	2.6
μ/D	16.1	15.5
$\beta/^\circ$ ^b	9	9
$\Delta\alpha/\text{\AA}^3$	25.1	25.8
$\alpha_{\text{avg}}/\text{\AA}^3$	44.3	44.8

^a Vacuum dipole moments obtained with the HF/6-31G(d) method and electronic polarizabilities at the B3LYP/3-21G level of theory. ^b Angle between the net dipole vector μ and μ_{\parallel} . For details see the ESI.

with concentration of **1** >2.5 mol% in **5CB**, 1.8 mol% in **6-CHBT**, and 2.7 mol% in **ZLI-1132** were not homogenous either in the isotropic phase or upon cooling to ambient temperature. Much greater solubility of **1** was observed in ester **CI Ester**,³⁹ and solutions up to 6 mol% were obtained. The solutions were apparently supersaturated, and after several weeks at ambient temperature some microcrystals of **1** were formed in solutions with concentration >2 mol%. The sulfonium derivative **2** exhibits greater solubility in organic solvents, and solutions up to nearly 10 mol% in **CI Ester** were obtained. This is consistent with the lower melting point of **2** as compared to **1**.

DSC analysis of the solutions in **CI Ester** demonstrated a linear increase of the clearing temperature T_{NI} with increasing concentration of **1** (Fig. 5). Extrapolation of data in Fig. 5 gave the virtual $[T_{\text{NI}}]$ for quinuclidinium **1** of 139 ± 1.3 °C. In contrast, solutions of sulfonium **2** in **CI Ester** exhibit a non-linear dependence of T_{NI} on concentration. The virtual temperature $[T_{\text{NI}}]$ calculated for **2** using the 9.5 mol% datapoint is 92 °C, which is nearly 50 K lower than $[T_{\text{NI}}]$ for **1**.

Dielectric measurements

The addition of small amounts of the zwitterion **1** or **2** to the **CI Ester** host possessing small negative dielectric anisotropy ($\Delta\epsilon = -0.59$) dramatically changed its dielectric properties (Fig. 6). The parallel component of dielectric permittivity, ϵ_{\parallel} , of the material significantly increased, while the perpendicular component, ϵ_{\perp} , was little affected by the additive (Fig. 6). In consequence, $\Delta\epsilon$ increased and the negative $\Delta\epsilon$ host was transformed to a positive $\Delta\epsilon$ material. The observed effect on the material's dielectric properties is consistent with the magnitude and orientation of the molecular dipole moment in the additive, and indicated good alignment in the nematic host. In addition,

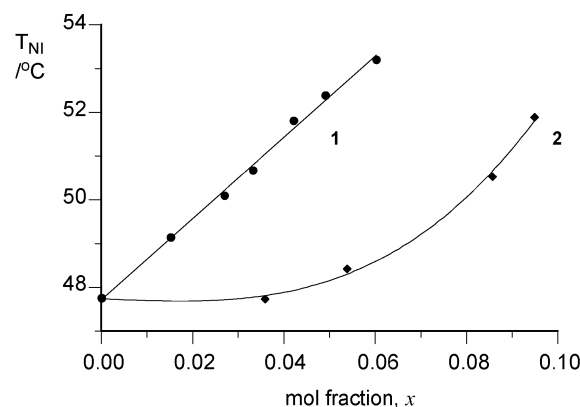
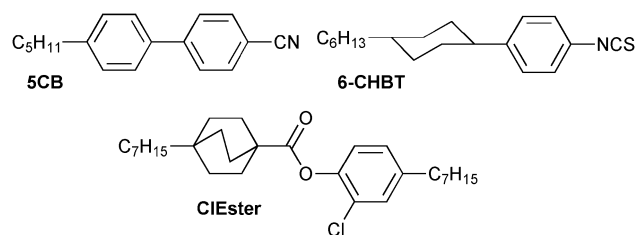


Fig. 5 A plot of peak temperature of the N–I transition for binary mixtures of quinuclidinium **1** (circles) and sulfonium **2** (diamonds) in **CI Ester**. Best fit line for **1**: $T_{\text{NI}} = 90.8(\pm 1.3)x + 47.8$.

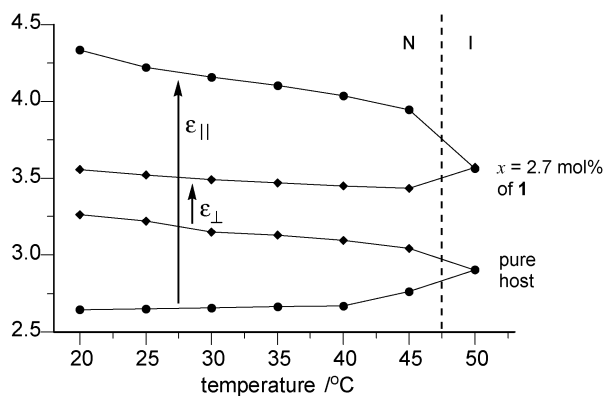


Fig. 6 Dielectric permittivity tensors ($\epsilon_{||}$ circles and ϵ_{\perp} diamonds) for the host, ClEster, and 2.7 mol% solution of **1** as a function of temperature. Estimated standard deviation for $\epsilon_{||}$ and ϵ_{\perp} is 0.1.

temperature dependence studies of dielectric parameters of one of the solutions demonstrated no anomalous behavior in the temperature range of the nematic phase (Fig. 6). Thus, the results indicate that both zwitterions **1** and **2** are compatible with the nematic host.

A plot of dielectric permittivity parameters measured for each solution at ambient temperature showed a non-linear dependence on concentration of the zwitterion (Fig. 7). This suggests a change of nature of the additive caused *e.g.* by aggregation.

Using equation 1, which reflects additive properties of dielectric permittivity, dielectric anisotropy $\Delta\epsilon$ of the pure zwitterion can be calculated for each individual concentration of **1** and **2** in ClEster. The resulting extrapolated $\Delta\epsilon$ values were fitted to a second-order polynomial⁴⁰ and the curves for quinuclidinium **1** and sulfonium **2** are shown in Fig. 8. Extrapolation to infinite dilution ($x \rightarrow 0$) yielded a $\Delta\epsilon$ value of 70 ± 1 for **1** and 61 ± 2 for **2**. Similar analysis for the $\epsilon_{||}$ component gave 88 ± 1 and 84 ± 1 for **1** and **2**, respectively.³⁷

Dielectric data analysis

Extrapolated dielectric data for **1** and **2** were analyzed quantitatively using the Maier-Meier equation,⁴¹ which relates bulk

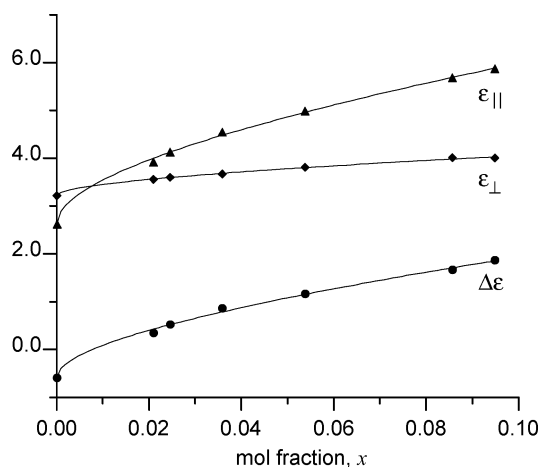


Fig. 7 Plot of $\epsilon_{||}$ (triangles), ϵ_{\perp} (diamonds), and $\Delta\epsilon$ (circles) vs concentration of **2** in ClEster at 25 °C.

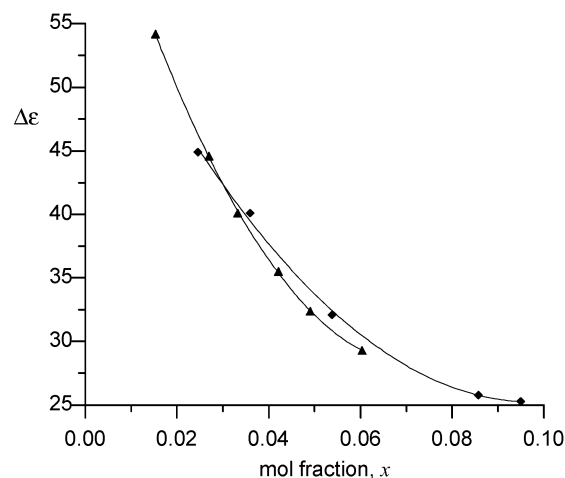


Fig. 8 Plot of extrapolated $\Delta\epsilon$ vs concentration of **1** (triangles) and **2** (diamonds) in ClEster fitted to a second-order polynomial.

parameters of the nematic phase, dielectric anisotropy $\Delta\epsilon$ and order parameter S , with molecular parameters, dipole moment μ and polarizability α (equation 2).⁴²

Considering the Maier-Meier relationship (equation 2) and results of dielectric measurements (*vide supra*), extrapolated dielectric parameters for the zwitterions depend on the Kirkwood factor⁴³ g (equation 3), apparent order parameter⁴⁴ S_{app} , temperature T , and concentration c . For $T = const$ and at a given concentration c of the additive, dielectric parameters $\epsilon_{||}$, ϵ_{\perp} , and $\Delta\epsilon$ depend on g and S_{app} . The two unknowns, S_{app} and g , were found for **1** and **2** by solving simultaneously the Maier-Meier expressions for $\epsilon_{||}$ and ϵ_{\perp} .³⁷

$$\Delta\epsilon = \sum_i x_i \Delta\epsilon_i \quad (1)$$

$$\Delta\epsilon = \frac{NFh}{\epsilon_0} \left\{ \Delta\alpha - \frac{F\mu_{eff}^2}{2k_B T} (1 - 3\cos^2\beta) \right\} S \quad (2)$$

$$\mu_{eff}^2 = g\mu^2 = \left(\frac{c-a}{c} \right) \mu^2 \quad (3)$$

$$K = \frac{[M_2]}{[M]} = \frac{a}{2(c-a)^2} \quad (4)$$

$$a = \frac{4Kc + 1 - \sqrt{8Kc + 1}}{4K} \quad (5)$$

$$g = \frac{\sqrt{8Kc + 1} - 1}{4Kc} \quad (6)$$

Initially, the medium was assumed to be the pure host, and the effect of the additive on dielectric properties of the solution was ignored. Analysis using dipole moments obtained in vacuum ($\epsilon = 1$) gave practically constant order parameter $S_{app} = 0.63 \pm 0.01$

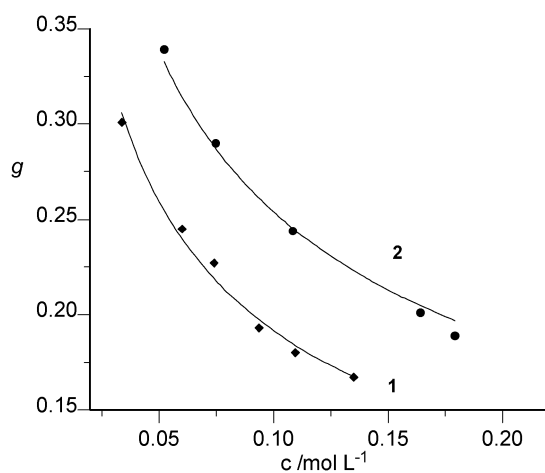


Fig. 9 A plot of calculated Kirkwood parameter g for **1** (diamonds) and **2** (circles) vs. concentration c . Dipole calculated at $\epsilon = 3.03$ (model 2). Fitting function shown as equation 6.

for **1** and $S_{app} = 0.50 \pm 0.01$ for **2** in the entire range of concentrations. The Kirkwood factor g was diminishing in a nonlinear mode from 0.38 to 0.21 for **1** and from 0.42 to 0.24 for **2** with increasing concentration of the additive. When larger dipole moments calculated for the dielectric medium of the host ($\epsilon = 3.03$) were used for the analysis, the order parameters remained the same, while the g factors were smaller by about 20% for both additives. A plot of resulting g values is shown in Fig. 9.³⁷

For comparison purposes dielectric parameters of the additives were calculated for ideal compatibility with ($S_{app} = S_{host} = 0.66$) and solubility ($g = 1$) in the host. The resulting dielectric values $\epsilon_{||}$ and $\Delta\epsilon$ for the pure zwitterions in **CI Ester** are 178 and 147, respectively, for quinuclidinium **1**, and 170 and 140 for sulfonium **2**. Calculations of S_{app} and g using dielectric parameters extrapolated to infinite dilution ($x = 0$, Fig. 8) gave 0.62 and 0.50 respectively for **1**, and 0.52 and 0.55 for **2**. The results indicate that the calculated dipole moments μ are overestimated by the HF computational method by about 30%.⁴⁵

Since the zwitterions significantly increase dielectric permittivity of the solutions, their dipole moments may vary with concentration. Also the reaction field parameters h and F (equation 2; see the ESI†) change appropriately with the increasing dielectric strength of the solution. Calculations using adjusted dipole moment of the additive and constant reaction field parameters demonstrated a drop in the value of the Kirkwood factor by about 10%. When all three parameters, μ , h , and F , were treated as a function of ϵ , the Kirkwood factor was smaller by an additional 5%. While the adjustments of these parameters affected the g factor, the apparent order parameter S_{app} for each zwitterion was practically unchanged.

The calculated small value of the Kirkwood factor demonstrates that a significant fraction of the zwitterions exist as aggregates, and the changing values of g indicate that the degree of aggregation increases with the increasing concentration of the additive. The observed aggregation of the zwitterion molecules **M** in dilute solutions can be approximated with a simple model of dimerization as shown in Scheme 3. Assuming that the dimer M_2 has no dipole moment, $\mu = 0$, the dielectric data can be used

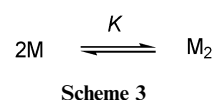


Table 3 Association constant K for **1** and **2**^a

Model	Parameters	K/L mol ⁻¹	
		1	2
1	μ for $\epsilon = 1$	63 ± 2	37 ± 1
2	μ for $\epsilon = 3.03$	110 ± 2.5	58 ± 1
3	μ for variable ϵ	122 ± 3	68 ± 3
4	μ , h , and F for variable ϵ	145 ± 5	89 ± 6

^a See text for details.

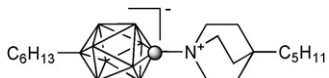
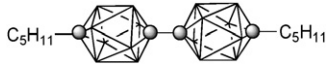

to calculate the constant K for the monomer-dimer equilibrium process shown in Scheme 3. At equilibrium, the concentration of the dimer M_2 is $0.5a$ and the monomer is $c - a$, where c is the concentration of the zwitterion in **CI Ester** solution expressed in mol/L. This leads to equation 4 for K , which is transformed to the expression for a (equation 5). The effective dipole moment μ_{eff}^2 is related to the dipole moment μ^2 by the Kirkwood factor g , which can be expressed as a fraction of monomeric molecules (equation 3). Substitution of equation 5 into equation 3 and solving for g leads to equation 6, in which g is a function of concentration c and K is the association constant.

Fitting the Kirkwood factors g obtained for values of μ calculated in vacuum (model 1 in Table 3) to the single parameter function (equation 6) gives the association constant K of 63 L/mol for quinuclidinium **1** and about a 40% smaller value, 37 L/mol, for the sulfonium **2**. For the g values calculated for the dielectric strength of the host (model 2, Table 3), the association constant K values are 75% and 57% bigger, respectively, due to larger calculated dipole moments for **1** and **2**. The constant K increased further when g was derived from adjustable dipole moments (model 3), and the largest, 145 L/mol and 89 L/mol for **1** and **2**, respectively, for g calculated with adjustable dipoles and reaction field parameters (model 4). Incidentally, the correlation factors for fitting data derived from adjustable parameters (models 3 and 4) to equation 6 are progressively worse than those for the fixed value of dipole moment values (models 1 and 2). This is reflected in higher uncertainty of the K values obtained in the former models as compared to those in models 1 and 2.

Discussion

The structure of the {*closo*-1-CB₉} cluster permits the design of anisometric molecules characterized by high compatibility with the nematic phase. This is evident from the high virtual clearing points, $[T_{NI}] > 90$ °C, and high apparent order parameters, $S_{app} >$

Table 4 N–I transition temperatures for selected compounds

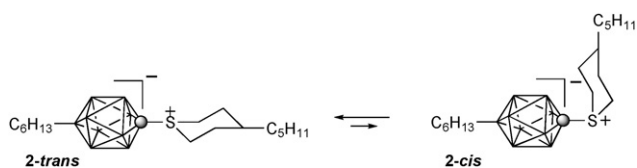
Compound	$[T_{NI}]^{d}/^{\circ}\text{C}$	$T_{NI}/^{\circ}\text{C}$
1 	138 ^b	^c
11 	75 ^d	98 ^d
12 	171 ^d	^e

^a Virtual N–I transition temperature. ^b Determined in **CI Ester** host. This work. ^c Not observed. ^d Ref. 46. ^e Sm–I transition at 244 °C; ref. 46.

0.5, for both additives in **CI Ester** host. The $[T_{NI}]$ for quinuclidinium **1** (139 °C) is higher by nearly 50 K than the $[T_{NI}]$ of sulfonium **2**, and favorably compares to $[T_{NI}]$ values for similar, non-polar two-ring compounds **11** and **12** measured in a different host (Table 4).⁴⁶ Interestingly, the $[T_{NI}]$ for **1** is close to an average of the $[T_{NI}]$ values for the two analogues **11** and **12**. Considering the difference in the alkyl chain length and that the measurements were performed in different hosts, the result indicates a rather modest effect of high dipole moment on phase stability.

The observed difference of 47 K in $[T_{NI}]$ values for the two zwitterions **1** and **2** is consistent with poorer alignment of molecules of the latter with the nematic director of the host than those of quinuclidinium **1**. Experimental results demonstrate that **1** aligns well with the host since the apparent order parameter, $S_{app} = 0.63$, is similar to that of the pure host ($S = 0.66$).³⁸ In contrast, the S_{app} value for sulfonium **2** is markedly lower (0.50).

The difference in behavior of the two zwitterions in a nematic phase is related, in part, to their conformational properties and the ability to adopt a co-planar orientation of the terminal alkyl chains. For the quinuclidinium **1** the two alkyl chains are 23° off co-planarity, while for the sulfonium **2** the inter-planar angle is nearly twice as large, according to *ab initio* modeling. The quinuclidinium **1** can, however, adopt an even more favorable configuration (11° inter-planar angle in the solid state) apparently without much thermodynamic penalty, as evident from the XRD analysis. Presumably, this greater conformational flexibility contributed to the higher $[T_{NI}]$ value of **1**. The high inter-planar angle calculated for **2** (43°) is similar to that calculated and observed experimentally⁴⁷ for alkyl derivatives of 10-vertex carborane derivative, such as **11** in Table 4, which is a consequence of the cage symmetry.^{21,47} It is presumably for this reason that binary mixtures involving many 10-vertex *closo*-borane derivatives, including **2** (Fig. 5), exhibit a non-linear concentration dependence of T_{NI} in the low mole fraction regions.^{46,48,49}

**Fig. 10** The *trans* and *cis* isomers of **2**.

Besides the unfavorable orientation of the terminal alkyl groups in the conformational ground state of **2**, epimerization at the sulfur center in **2** and the formation of the *cis* isomer (**2-cis**, Fig. 10) may also contribute to the low dynamic anisotropy of the molecule, and, consequently, lower $[T_{NI}]$ value as compared to **1**. Such epimerization and *cis/trans* equilibrium shown for **2** in Fig. 10 is anticipated on the basis of our findings for another 10-vertex cluster derivative.⁵⁰

Both compounds **1** and **2** have significant dipole moments oriented along the long molecular axis. This, considering their good alignment with the nematic director, renders both compounds as highly effective positive $\Delta\epsilon$ additives. For instant, 1 mol% concentration of the zwitterion increases $\Delta\epsilon$ of the **CI Ester** host by about +0.60 for **1** and +0.54 for **2**. Unfortunately, both compounds have rather low solubility in typical nematic hosts, and their possible applications in electrooptical devices will require structural modifications. Analysis of the two zwitterions demonstrates that lowering the symmetry of **1** to that of **2** decreases the melting point by about 150 K, increases solubility by nearly 2 fold, and also lowers the tendency to association (lower K value). Thus, further dissymmetrization of **2**, by *e.g.* modifying the alkyl chains, is expected to improve the solubility without significantly compromising its effectiveness as a high $\Delta\epsilon$ additive.

The Maier-Meier analysis provides a convenient method for quantitative understanding of the behavior of the additives in solutions. As we already demonstrated for other binary mixtures,^{26,51} the calculated apparent order parameter S_{app} indicates the degree of alignment of the additive with the nematic director, and hence its steric compatibility with the host. In previous analyses,^{26,51} the dielectric parameters were changing linearly with the concentration of the additive giving a constant value of the Kirkwood factor g . The non-linear behavior of the dielectric data for solutions of **1** and **2**, and consequently variable Kirkwood factor g , indicate aggregation of the solute, which is expected for highly polar compounds in weakly polar media. Unlike in previous studies, the effect of **1** and **2** on the dielectric properties of the solution is substantial and proper analysis of the data may require inclusion of the dielectric effect of the additive on μ and reaction field parameters h and F . As the calculated dipole increases in the higher dielectric strength medium, the additives are more associated and smaller Kirkwood factors g are obtained.

Further analysis demonstrated that for hypothetical ideal solutions of **1** and **2** in **CI Ester** (high order parameter, $S_{app} = S_{host}$, and no aggregation, $g = 1$) the dielectric parameters of the pure additives are about twice as large as those extrapolated to infinite dilution ($x \rightarrow 0$) from the real solutions. This is in part due to the lower S_{app} of the additives and in part to apparent overestimation of the dipole moment at the HF level of theory.⁴⁵ Assuming that the extrapolated dielectric values are reliable, the actual dipole moment of **1** and **2** is about 11 D.

Since the Kirkwood factor g derived from the Maier-Meier equation is related to the fraction of non-associated molecules, it can be used to calculate the association constant K for a simple dimerization process. The actual molecular process leading to lowering the effective dipole moment is presumably more complex; it may involve a larger number of molecules in the aggregates and incomplete compensation of the dipole moment especially at higher concentrations.⁵² Nevertheless, such

a simplistic treatment of the molecular association provides a convenient and quantitative description of non-linear dielectric systems such as solutions of **1** and **2** in **CI Ester**. Moreover, the calculated association constant K offers a means for quantitative comparison of different highly polar additives. Out of the four models of treatment of the molecular dipole moment of the additive (Table 3), the most complete, but also most expensive computationally, appears to be model 4 in which all three parameters, μ , h and F , are functions of the additive's concentration. However, for the practical purpose of comparing the behavior of various polar additives, the simplest model involving the molecular dipole moment calculated in vacuum is appropriate.

Summary and conclusions

Synthetic access to a new class of highly effective, low concentration, positive dielectric anisotropy additives to nematic materials has been developed. The first two examples, zwitterions **1** and **2**, have been prepared and characterized in a nematic host. Solution dielectric data were analyzed with the aid of the Maier-Meier relationship and quantum-mechanical calculations, which provided a convenient protocol for the quantitative understanding of the behavior of polar additives in solutions and for the comparison of their properties. Data indicate that quinuclidinium **1** exhibits higher compatibility with the nematic phase (higher apparent order parameter S_{app} and higher $[T_{NI}]$) than the sulfonium **2**. However, the sulfonium **2** is more soluble and has a markedly lower association constant K .

Further tailoring of the properties of this class of zwitterions for practical applications will involve structural modification of **1** and **2** to increase their solubility.

Computational details

Quantum-mechanical calculations were carried out using the Gaussian 98⁵³ suite of programs. Geometry optimizations for unconstrained conformers of **1** and **2** with the most extended molecular shapes were undertaken at the HF/6-31G(d) and B3LYP/3-21G levels of theory using default convergence limits. Dipole moments of **1** and **2** for analysis with the Maier-Meier theory were obtained using the HF/6-31G(d) method, and exact electronic polarizabilities were calculated at the B3LYP/3-21G level of theory. The latter are considered to be underestimated by about 10%. Dipole moment components μ and polarizability tensors α were calculated in Gaussian standard orientation of each molecule (charge based), which is close to the principal moment of inertia coordinates (mass based). The IPCM solvation model⁵⁴ was used with default parameters to obtain molecular dipole moment components for dielectric strength ϵ of the medium: 2.84, 3.03, 4.00, and 4.62. The resulting linear dependence $\mu(\epsilon)$ was used to calculate molecular dipole moments of the additive for each solution.

Experimental

Binary mixtures preparation

Solutions of **1** or **2** in host **CI Ester** (~10 mg) were prepared in an open vial with agitation using a closed-end capillary tube with moderate heating supplied by a heat gun. The binary mixtures

were analyzed by polarized optical microscopy (POM) to ensure that the mixtures were homogeneous. The mixtures were then allowed to condition for 3 hr at room temperature. The clearing temperature of each homogeneous mixture was determined by DSC as the peak of the transition.

Electrooptical measurements

Dielectric properties of solutions of zwitterions **1** and **2** in **CI Ester** were measured by a Liquid Crystal Analytical System (LCAS - Series II, LC Analytical Inc.) using GLCAS software version 0.951, which implements literature procedures for dielectric constants.⁵⁵ The homogeneous binary mixtures were loaded into ITO electrooptical cells by capillary forces with moderate heating supplied by a heat gun. The cells (about 4 μm thick, electrode area of 0.581 cm^2 and anti-parallel rubbed polyimide layer 2°–3° pretilt) were obtained from LCA Inc., and their precise thickness ($\pm 0.05 \mu\text{m}$) was measured by LCAS using the capacitance method before the cells were filled. The filled cells were heated to an isotropic phase and were cooled to room temperature before measuring the dielectric properties. Default parameters were used for measurements: triangular shaped voltage bias ranging from 0.1–20 V at 1 kHz frequency. The threshold voltage V_{th} was measured at a 10% change. For each mixture, the measurement was repeated seven times for two cells. The first two measurements for each cell were discarded as conditioning measurements, and the remaining total ten results were averaged to calculate the mixture's parameters. Dielectric parameters of the pure host **CI Ester** were measured in similar cells in which the electrode area (0.28 cm^2) was covered with a surfactant to impose a homeotropic alignment.

The results are collected in Tables S3 and S4 in ESI.†

Acknowledgements

Financial support for this work was received from the National Science Foundation (DMR-0606317). XRD results were obtained using ChemMatCARS Sector 15, which is principally supported by the NSF/DoE under grant number CHE-0535644, the Advanced Photon Source, which is supported by the U. S. Department of Energy, Office of Science, Office of Basic Energy Sciences, under Contract No. DE-AC02-06CH11357. We thank Prof. R. Dabrowski for his generous gift of **CI Ester**.

References

- 1 I. C. Sage in *Handbook of Liquid Crystals*; Demus, D., Goodby, J. W., Gray, G. W., Spiess, H.-W., Vill, V., Eds.; Wiley-VCH: New York, 1998; Vol. 1, p 731–762.
- 2 P. Kirsch and M. Bremer, *Angew. Chem., Int. Ed.*, 2000, **39**, 4216–4235.
- 3 V. Fréedericksz and V. Zolina, *Trans. Faraday Soc.*, 1933, **29**, 919–930.
- 4 L. M. Blinov, V. G. Chigrinov *Electrooptic Effects in Liquid Crystal Materials*; Springer-Verlag: New York, 1994.
- 5 L. M. Blinov in *Handbook of Liquid Crystals*; Demus, D., Goodby, J. W., Gray, G. W., Spiess, H.-W., Vill, V., Eds.; Wiley-VCH: New York, 1998; Vol. 1, p 477–534.
- 6 For example: G. W. Gray, K. J. Harrison and J. A. Nash, *Electron. Lett.*, 1973, **9**, 130–131; R. Eidenschink, D. Erdmann, J. Krause and L. Pohl, *Angew. Chem., Int. Ed. Engl.*, 1977, **16**, 100.
- 7 R. Dabrowski, J. Dziaduszek and T. Szczucinski, *Mol. Cryst. Liq. Cryst.*, 1984, **102**, 155–160; R. Dabrowski and J. Dziaduszek, *Mol. Cryst. Liq. Cryst.*, 1985, **124**, 241–257; R. Dabrowski,

- J. Dziaduszek, W. Drzewinski, K. Czuprynski and Z. Stolarz, *Mol. Cryst. Liq. Cryst.*, 1990, **191**, 171–176.
- 8 For example: H. Zschke, *J. Prakt. Chem.*, 1975, **317**, 617–630; G. Kraus and H. Zschke, *J. Prakt. Chem.*, 1981, **323**, 199–206.
- 9 H.-M. Vorbrod, S. Deresch, H. Kresse, A. Wiegeleben, D. Demus and H. Zschke, *J. Prakt. Chem.*, 1981, **323**, 902–913.
- 10 D. Demus in *Handbook of Liquid Crystals*; Demus, D., Goodby, J. W., Gray, G. W., Spiess, H.-W., Vill, V., Eds.; Wiley-VCH: New York, 1998; Vol. 1, p 133–187.
- 11 K. J. Toyne in *Thermotropic Liquid Crystals*; Gray, G. W., Ed.; Wiley: New York, 1987; pp 28–63, and references therein.
- 12 K. Wohlfart, M. Schnell, J.-U. Grabow and J. Küpper, *J. Mol. Spectrosc.*, 2008, **247**, 119–121.
- 13 W. J. McKillip, E. A. Sedor, B. M. Culbertson and S. Wawzonek, *Chem. Rev.*, 1973, **73**, 255–281.
- 14 C. Serbutoviez, J.-F. Nicoud, J. Fischer, I. Ledoux and J. Zyss, *Chem. Mater.*, 1994, **6**, 1358–1368.
- 15 E. Alcalde, L. Pérez, J. P. Fayet and M. C. Vertut, *Chem. Lett.*, 1991, 845–848 and references therein.
- 16 B. Künkemeier-Schröder, A.-C. Koch, G. Pelzl and W. Friedrichsen, *Liq. Cryst.*, 1993, **15**, 559–561.
- 17 C. V. Yelamaggad, M. Mathews, U. S. Hiremath, D. S. S. Rao and S. K. Prasad, *Tetrahedron Lett.*, 2005, **46**, 2623–2626; C. V. Yelamaggad, M. Mathews, U. S. Hiremath, D. S. S. Rao and S. K. Prasad, *Chem. Commun.*, 2005, 1552–1554.
- 18 H. Kise, Y. Nishisaka, T. Asahara and M. Seno, *Chem. Lett.*, 1978, 1235–1238.
- 19 P. Kaszynski, J. Huang, G. S. Jenkins, K. A. Bairamov and D. Lipiak, *Mol. Cryst. Liq. Cryst.*, 1995, **260**, 315–332.
- 20 P. Kaszynski, D. Lipiak in *Materials for Optical Limiting*; Crane, R., Lewis, K., Stryland, E. V., Khoshnevisan, M., Eds.; MRS: Boston, 1995; Vol. 374, p 341–347.
- 21 P. Kaszynski and A. G. Douglass, *J. Organomet. Chem.*, 1999, **581**, 28–38 and references therein.
- 22 P. Kaszynski, S. Pakhomov and V. G. Young Jr, *Collect. Czech. Chem. Commun.*, 2002, **67**, 1061–1083; S. Pakhomov, P. Kaszynski and V. G. Young Jr, *Inorg. Chem.*, 2000, **39**, 2243–2245; A. Balinski, A. Januszko, J. E. Harvey, E. Brady, P. Kaszynski, V. G. Young Jr., in preparation; P. Kaszynski, in *Anisotropic Organic Materials*; R. Glaser and P. Kaszynski, Eds.; ACS Symposia: Washington D.C., 2001; Vol. 798, p 68–82.
- 23 A. Januszko, P. Kaszynski, M. D. Wand, K. M. More, S. Pakhomov and M. O'Neill, *J. Mater. Chem.*, 2004, **14**, 1544–1553; M. Jasinski, A. Jankowiak, A. Januszko, M. Bremer, D. Pauluth and P. Kaszynski, *Liq. Cryst.*, 2008, **35**, 343–350.
- 24 K. Ohta, A. Januszko, P. Kaszynski, T. Nagamine, G. Sasnouski and Y. Endo, *Liq. Cryst.*, 2004, **31**, 671–682; A. Januszko and P. Kaszynski, *Liq. Cryst.*, 2008, **35**, 705–710.
- 25 For other recent publications see: B. Ringstrand, J. Vroman, D. Jensen, A. Januszko, P. Kaszynski, J. Dziaduszek and W. Drzewinski, *Liq. Cryst.*, 2005, **32**, 1061–1070; A. Januszko, K. L. Glab and P. Kaszynski, *Liq. Cryst.*, 2008, **35**, 549–553; T. Nagamine, A. Januszko, K. Ohta, P. Kaszynski and Y. Endo, *Liq. Cryst.*, 2008, **35**, 865–884.
- 26 A. Januszko, K. L. Glab, P. Kaszynski, K. Patel, R. A. Lewis, G. H. Mehl and M. D. Wand, *J. Mater. Chem.*, 2006, **16**, 3183–3192.
- 27 B. Ringstrand, A. Balinski, A. Franken and P. Kaszynski, *Inorg. Chem.*, 2005, **44**, 9561–9566.
- 28 B. Ringstrand, P. Kaszynski and H. Monobe, *J. Mater. Chem.*, 2009, **19**, 4805–4812.
- 29 K. A. Bairamov, A. G. Douglass and P. Kaszynski, *Synth. Commun.*, 1998, **28**, 527–540.
- 30 B. Ringstrand, P. Kaszynski and A. Franken, *Inorg. Chem.*, 2009, **48**, 7313–7329.
- 31 J. Thomas and D. Clough, *J. Pharm. Pharmacol.*, 1963, **15**, 167–177; N. P. Volynskii and L. P. Shcherbakova, *Bull. Acad. Sci. USSR, Div. Chem. Sci. (Engl. Transl.)*, 1979, **28**, 1006–1009.
- 32 Crystal data for **1** (CCDC 731853): C₁₉H₄₄B₉N triclinic, P-1, *a* = 9.766(2) Å, *b* = 10.481(3) Å, *c* = 12.098(3) Å, α = 93.804(9)°, β = 90.249(10)°, γ = 102.587(10)°, *V* = 1205.7(5) Å³, *Z* = 2, *T* = 95(2) K, λ = 0.49595 Å, *R*(F₂) = 0.0641 or *R*_w(F₂) = 0.1789 (for 3664 reflections with *I* > 2σ(*I*)).
- 33 T. Jelinek, B. Stibr, J. Plešek, M. Thornton-Pett and J. D. Kennedy, *J. Chem. Soc., Dalton Trans.*, 1997, 4231–4236.
- 34 A. G. Douglass, Z. Janousek, P. Kaszynski and V. G. Young, Jr, *Inorg. Chem.*, 1998, **37**, 6361–6365.
- 35 The pyramidalization angle α is defined as the N–C–* angle, where * represents the mid-point between the carbon atoms adjacent to N.
- 36 P. Kaszynski, S. Pakhomov, M. E. Gurskii, S. Y. Erdyakov, Z. A. Starikova, K. A. Lyssenko, M. Y. Antipin, V. G. Young Jr. and Y. N. Bubnov, *J. Org. Chem.*, 2009, **74**, 1709–1720.
- 37 For details see the Electronic Supplementary Information† (ESI).
- 38 S. Urban, J. Kedzierski and R. Dabrowski, *Z. Naturforsch.*, 2000, **55A**, 449–456.
- 39 R. Dabrowski, J. Jadzyn, S. Czerkas, J. Dziaduszek and A. Walczak, *Mol. Cryst. Liq. Cryst.*, 1999, **332**, 61–68.
- 40 The data can more properly be fitted to a hyperbolic function such as $y = a/(x + b)$ giving slightly bigger extrapolated dielectric values with significantly higher uncertainty. The Maier-Meier calculations using these extrapolated dielectric parameters give *g* values that are very similar to those obtained from the quadratic function extrapolation. The polynomial appears to describe well the dielectric data for *x* < 0.1. More in the ESI†.
- 41 W. Maier and G. Meier, *Z. Naturforsch.*, 1961, **16A**, 262–267, and 470–477.
- 42 S. Urban in *Physical Properties of Liquid Crystals: Nematics*, D. Dunmur, A. Fukuda, and G. Luckhurst, Eds; IEE, London, 2001, pp 267–276.
- 43 P. Bordewijk, *Physica*, 1974, **75**, 146–156.
- 44 Local orientational parameter of the additive in the host.
- 45 The dipole moment for the [*closo*-CH₁₁H₁₁-12-C₇H₆] zwitterion is calculated as 14.3 D in benzene dielectric medium (HF/6-31G(d) method), while the measured value is 11.25 D: B. Grüner, Z. Janoušek, B. T. King, J. N. Woodford, C. H. Wang, V. Všetěčka and J. Michl, *J. Am. Chem. Soc.*, 1999, **121**, 3122–3126.
- 46 W. Piecek, J. M. Kaufman and P. Kaszynski, *Liq. Cryst.*, 2003, **30**, 39–48.
- 47 P. Kaszynski, S. Pakhomov, K. F. Tesh and V. G. Young, Jr, *Inorg. Chem.*, 2001, **40**, 6622–6631.
- 48 A. G. Douglass, B. Both and P. Kaszynski, *J. Mater. Chem.*, 1999, **9**, 683–686.
- 49 K. Czuprynski and P. Kaszynski, *Liq. Cryst.*, 1999, **26**, 775–778.
- 50 A. Miniewicz, A. Samoc, M. Samoc and P. Kaszynski, *J. Appl. Phys.*, 2007, **102**, 033108.
- 51 T. Nagamine, A. Januszko, P. Kaszynski, K. Ohta and Y. Endo, *J. Mater. Chem.*, 2006, **16**, 3836–3843.
- 52 For instance: P. Kedziora and J. Jadzyn, *Acta Phys. Polon. A*, 1990, **A77**, 605–610; P. Kedziora and J. Jadzyn, *Mol. Cryst. Liq. Cryst.*, 1990, **192**, 31–37.
- 53 *Gaussian 98, Revision A.7*, M. J. Frisch, G. W. Trucks, H. B. Schlegel, G. E. Scuseria, M. A. Robb, J. R. Cheeseman, V. G. Zakrzewski, J. A. Montgomery, Jr., R. E. Stratmann, J. C. Burant, S. Dapprich, J. M. Millam, A. D. Daniels, K. N. Kudin, M. C. Strain, O. Farkas, J. Tomasi, V. Barone, M. Cossi, R. Cammi, B. Mennucci, C. Pomelli, C. Adamo, S. Clifford, J. Ochterski, G. A. Petersson, P. Y. Ayala, Q. Cui, K. Morokuma, D. K. Malick, A. D. Rabuck, K. Raghavachari, J. B. Foresman, J. Cioslowski, J. V. Ortiz, A. G. Baboul, B. B. Stefanov, G. Liu, A. Liashenko, P. Piskorz, I. Komaromi, R. Gomperts, R. L. Martin, D. J. Fox, T. Keith, M. A. Al-Laham, C. Y. Peng, A. Nanayakkara, C. Gonzalez, M. Challacombe, P. M. W. Gill, B. Johnson, W. Chen, M. W. Wong, J. L. Andres, C. Gonzalez, M. Head-Gordon, E. S. Replogle, and J. A. Pople, Gaussian, Inc., Pittsburgh PA, 1998.
- 54 J. B. Foresman, T. A. Keith, K. B. Wiberg, J. Snoonian and M. J. Frisch, *J. Phys. Chem.*, 1996, **100**, 16098–16104.
- 55 S. T. Wu, D. Coates and E. Bartmann, *Liq. Cryst.*, 1991, **10**, 635–646.